JOURNAL OF VIROLOGY, Aug. 2010, p. 8007–8020 Vol. 84, No. 16
0022-538X/10/$12.00 doi:10.1128/JVI.00334-10
Copyright © 2010, American Society for Microbiology. All Rights Reserved.

Multiple DNA Damage Signaling and Repair Pathways Deregulated by Simian Virus 40 Large T Antigen▽

Sergei Boichuk, Liang Hu, Jennifer Hein, and Ole V. Gjoerup*

Cancer Virology Program, University of Pittsburgh Cancer Institute, Pittsburgh, Pennsylvania 15213

Received 12 February 2010/Accepted 27 May 2010

We demonstrated previously that expression of simian virus 40 (SV40) large T antigen (LT), without a viral origin, is sufficient to induce the hallmarks of a cellular DNA damage response (DDR), such as focal accumulation of γ-H2AX and 53BP1, via Bub1 binding. Here we expand our characterization of LT effects on the DDR. Using comet assays, we demonstrate that LT induces overt DNA damage. The Fanconi anemia pathway, associated with replication stress, becomes activated, since FancD2 accumulates in foci, and mono-ubiquitinated FancD2 is detected on chromatin. LT also induces a distinct set of foci of the homologous recombination repair protein Rad51 that are colocalized with Nbs1 and PML. The FancD2 and Rad51 foci require neither Bub1 nor retinoblastoma protein binding. Strikingly, wild-type LT is localized on chromatin at, or near, the Rad51/PML foci, but the LT mutant in Bub1 binding is not localized there. SV40 infection was previously shown to trigger ATM activation, which facilitates viral replication. We demonstrate that productive infection also triggers ATR-dependent Chk1 activation and that Rad51 and FancD2 colocalize with LT in viral replication centers. Using small interfering RNA (siRNA)-mediated knockdown, we demonstrate that Rad51 and, to a lesser extent, FancD2 are required for efficient viral replication *in vivo*, suggesting that homologous recombination is important for high-level extrachromosomal replication. Taken together, the interplay of LT with the DDR is more complex than anticipated, with individual domains of LT being connected to different subcomponents of the DDR and repair machinery.

Simian virus 40 (SV40) carries genes encoding three early proteins: large T antigen (LT), small t antigen, and 17k. LT has served as a powerful model system for understanding cellular processes, such as DNA replication and malignant transformation (1, 16). An *in vitro* SV40 replication system based on purified cellular factors was established long ago, which in many ways recapitulates *in vivo* replication (33, 71). However, although very insightful, certain aspects of DNA replication cannot be reconstructed in a test tube and remain incompletely understood. Since SV40 relies extensively on cellular replication factors, it must reprogram the cellular environment to support viral DNA replication. A key component is cell cycle reprogramming, perhaps most importantly the potent induction of S phase in quiescent cells (19).

The ability of LT to induce aberrant cellular proliferation depends on binding to and inactivating key tumor suppressors like p53 and the retinoblastoma protein (pRB) family (reviewed in references 1 and 16). These interactions are also critical for oncogenic transformation and induction of tumors in a wide variety of cell types and tissues. Additional functions contribute to transformation. A functional DnaJ domain resides within the first 70 amino acids, which directs binding of the Hsc70 molecular chaperone and contributes to both oncogenic transformation and viral replication proficiency (10, 59). Distinct binding sites for a Cul7 ubiquitin ligase complex and the Bub1 mitotic checkpoint kinase are found immediately downstream of the DnaJ domain, and both binding proteins contribute to malignant transformation induced by LT (2, 17).

Efficient viral replication *in vivo* depends not only on LT-induced S-phase entry. Recent studies have illuminated how viruses target the DNA damage response (DDR) (reviewed in references 14 and 35). The DDR can be divided into two major branches according to the lesions that are sensed. Double-strand breaks (DSBs) are known to activate the ATM (ataxia-telangiectasia mutated) kinase, which in turn triggers cell cycle checkpoints to halt the cell cycle and promote DNA repair. Conversely, lesions with single-stranded DNA (ssDNA), for example arising from replication stress, trigger ATR (ataxia-telangiectasia and Rad3-related) kinase activation.

DSBs are a serious threat to genomic stability. When DSBs arise, they are sensed by the MRN (Mre11-Rad50-Nbs1) complex that triggers ATM-mediated phosphorylation of histone H2AX (referred to as γ-H2AX) in the flanking chromatin (32, 50). Strikingly, γ-H2AX accumulates in characteristic nuclear foci that are often considered a surrogate marker of DSBs (52). These foci are believed to be fundamentally important for retention of repair proteins at the break site and possibly checkpoint signaling (5, 63). DSBs can be repaired by either one of two distinct repair pathways, nonhomologous end joining (NHEJ) or homologous recombination (HR). A key component of the HR machinery is the Rad51 protein, which is also recruited to subnuclear foci to orchestrate repair (5, 26, 41, 42, 51). A subset of foci is composed of ssDNA, arising from resection of a DSB or from stalled replication forks. The ssDNA is coated by replication protein A (RPA), which subsequently recruits ATR and its obligate partner ATRIP (ATR-interacting protein). The Fanconi anemia pathway is involved in recognition and repair of stalled replication forks or other

* Corresponding author. Mailing address: Hillman Cancer Center, Research Pavilion Suite 1.8, 5117 Centre Avenue, Pittsburgh, PA 15213. Phone: (412) 623-7717. Fax: (412) 623-7715. E-mail: ovg27@pitt.edu.

▽ Published ahead of print on 2 June 2010.

kinds of replication stress (26, 29, 44). Fanconi anemia, together with other genetic disorders, such as Nijmegen breakage syndrome (Nbs1) and breast cancer 1 (BRCA1), are striking examples that loss of genomic stability through compromise of DNA repair pathways can directly contribute to human malignancies.

Some viruses, like adenovirus, dismantle the DDR via expression of specific viral proteins (14, 35, 62). In contrast, SV40 and mouse polyomavirus exploit the DDR by activating the DDR and benefiting from it (18, 23, 54, 76). SV40 infection leads to activation of the ATM kinase and downstream components, such as γ-H2AX, p53, and Chk2 (54, 76). The MRN complex is recruited to viral replication centers together with LT, RPA, and in close proximity, the PML protein. PML, a tumor suppressor, nucleates the formation of PML oncogenic domains known to participate in a diverse array of cellular functions, such as antiviral defenses, DNA damage repair, apoptosis, and transcriptional regulation (6). Late in infection, the MRN complex is, at least partially, degraded via Cul7 (76). Genetic loss of ATM or inhibition of ATM kinase substantially compromises viral replication and virion production, concomitant with the disappearance of replication centers and lack of MRN degradation. It was suggested that SV40 might have commandeered an intrinsic cellular DNA repair pathway to carry out its replication, since it appears to have usurped many of the factors involved (76). Nevertheless, it remains poorly understood mechanistically exactly how DDR activation can promote viral replication.

Our recent observations have indicated that expression of LT alone, in the absence of a viral replication origin, is sufficient to induce hallmarks of the ATM/ATR-mediated DDR, such as large γ-H2AX/53BP1 foci, p53 phosphorylation/stabilization, and Chk1/2 kinase activation in human BJ/tert fibroblasts (23). This response depends primarily on Bub1 binding and can be efficiently induced by an pRB binding-deficient 17k protein, which shares the first 131 amino acids with LT but ends in four unique residues.

In this study, we have significantly extended the analysis of mechanisms and consequences of DDR perturbations by LT. Comet assays demonstrate that LT induces overt DNA damage. We discovered further complexities in the DDR signaling and DNA repair elements influenced by LT. Thus, LT induces activation of the Fanconi anemia protein FancD2 by relocalizing it into foci on chromatin, a process normally linked to replication stress, for example, from stalled replication forks (26, 44). LT also induces distinct foci of the HR repair protein Rad51, which are colocalized with Nbs1 and PML. Both FancD2 and Rad51 foci are induced by LT independent of Bub1 and pRB binding. LT, but not the Bub1-binding mutant, is localized in foci juxtaposed with Rad51 and PML. Complementing previous studies that showed ATM activation following SV40 infection (54, 76), we find that Chk1 is activated through the ATR pathway. During viral infection, both FancD2 and Rad51 colocalize with LT in replication centers, and small interfering RNA (siRNA)-mediated downregulation of FancD2 or Rad51 causes an impairment of SV40 origin-dependent replication *in vivo*.

MATERIALS AND METHODS

Cell culture. BJ/tert fibroblasts stably expressing empty vector, LT, or its mutants were grown in 80% Dulbecco's modified Eagle's medium (Lonza) and 20% medium 199 (Invitrogen) supplemented with 10% fetal calf serum (FCS) (HyClone) and 1% penicillin-streptomycin (Invitrogen). GM07166 tert cells (74) (Nbs1 deficient, kindly provided by X. Wu, The Scripps Research Institute) as well as monkey kidney epithelial BSC40 cells (kindly provided by J. Pipas, University of Pittsburgh) and COS-1 cells were cultured in DMEM with 10% FCS and 1% penicillin-streptomycin. All cells were cultured at 37°C in a humidified incubator containing 5% CO_2.

Plasmids and transfection. Retroviral vectors (pLNBCX) expressing wild-type LT or the dl89-97 mutant were previously described (23). The pRB-binding mutant of LT (K1) was generated by site-directed mutagenesis of pLBNCX LT.

siRNAs for ATM, ATR, FancD2, or Rad51 (SMARTpool; Dharmacon), or a nontargeting control siRNA, were transfected into COS-1 or BSC40 cells using Lipofectamine RNAiMAX reagent according to the manufacturer's protocol (Invitrogen). Although SMARTpool siRNAs were designed against the human sequences, we found that they efficiently silenced expression of the homologous monkey proteins. Cy3-labeled siRNA indicated that >90% of cells were transfected. Plasmid DNA was transfected by Fugene-6 (Roche).

Viral infections. Retroviral vectors were transiently transfected into Phoenix amphotropic packaging cell line using the calcium phosphate precipitation method (15, 23). At 48 h posttransfection, the virus-containing supernatant was harvested, filtered through a 0.45-μm membrane (Millipore), aliquoted, and stored at −80°C. Cells were infected with 1 ml of virus supernatant in the presence of Polybrene (8 μg/ml). After 48 h, the infected cells were passed and continued to grow under blasticidin (5 μg/ml) selection for 5 to 7 days.

SV40 infections were performed essentially as previously outlined (76).

Antibodies and inhibitors. Primary mouse monoclonal antibodies were purchased from BD Biosciences (Orc2 clone 920-4-41), Millipore (Rad51 clone 3C10), Oncogene (BRCA1 clone Ab-1), Rockland (pATM S1981 200-301-400), Santa Cruz (PML clone PG-M3, cyclin A clone 6E6, BRCA1 D-9), and Sigma (α-tubulin clone B-5-1-2). Monoclonal antibodies against LT (PAb416, PAb419, and PAb423) and rabbit polyclonal antibody against ATRIP were previously described (23). Antibody to polymerase α (SJK132-20) was kindly provided by Ellen Fanning. Primary rabbit polyclonal antibodies were purchased from Bethyl Laboratories (RPA32 A300-244A and pRPA S4/8 A300-245A), Calbiochem (53BP1 Ab-1), Chemicon (PML AB1370), Genetex (FancD2 GTX30142), Novus Biologicals (Nbs1 NB100-143, Mre11 NB100-142, and ATR NB100-323), R&D Systems (pChk1 S317, pChk2 T68), and Santa Cruz (SV40 LT [v-300], p53 [FL-393], and Rad51 [H-92]). ATM and pATM S1981 rabbit monoclonal antibodies were from Epitomics. Secondary antibodies for immunofluorescence staining were obtained from Invitrogen (Alexa Fluor 488-labeled antibodies) and Jackson ImmunoResearch (Cy3-labeled antibodies). ATM inhibitor (KU55933) was purchased from Tocris Bioscience and used at a final concentration of 10 μM.

Cellular fractionation and Western blotting. Whole-cell extracts were prepared as previously described (23). In brief, the cells were washed in ice-cold phosphate-buffered saline (PBS) and lysed with TEB buffer (20 mM Tris [pH 7.5], 137 mM NaCl, 10% glycerol, 1% Nonidet P-40) supplemented with protease and phosphatase inhibitors. Some samples were extracted in radioimmunoprecipitation assay (RIPA) buffer (50 mM Tris [pH 8.0], 150 mM NaCl, 1% Nonidet P-40, 0.5% sodium deoxycholate, 0.1% sodium dodecyl sulfate [SDS]). The samples were resolved on 4 to 12% Bis-Tris or 3 to 8% Tris-acetate NuPAGE gels (Invitrogen), transferred to a nitrocellulose membrane (Bio-Rad), probed with specific antibody, and visualized by enhanced chemiluminescence (Western Lightning Plus-ECL reagent). Western blot images were processed using Adobe Photoshop 7.0, and bands were quantitated using ImageJ software.

Chromatin fractionation was performed essentially by the method of Mendez and Stillman (40). Briefly, the cells were resuspended in buffer A (10 mM HEPES [pH 7.9], 10 mM KCl, 1.5 mM $MgCl_2$, 10 mM NaF, 340 mM sucrose, 10% glycerol, 0.1% Triton X-100) supplemented with protease/phosphatase inhibitors and 1 mM dithiothreitol (DTT) and incubated on ice for 5 min. The nuclear pellet was collected by low-speed centrifugation, washed in buffer A, and subsequently lysed in buffer B (3 mM EDTA, 0.2 mM EGTA) while incubating on ice for 10 min. The insoluble chromatin was collected by centrifugation, resuspended in SDS sample buffer, sonicated, and boiled.

Immunofluorescence. BJ/tert cell lines were seeded on glass coverslips (Fisher) coated with poly-L-lysine (Sigma) and cultured for the next 48 h. The cells were washed twice with ice-cold PBS and fixed at 4°C for 15 min with 4% paraformaldehyde (Electron Microscopy Sciences, PA). In some cases, before

the cells were fixed, the slides were preextracted with CSK buffer [10 mM piperazine-*N*,*N*′-bis(2-ethanesulfonic acid) (PIPES) (pH 7), 100 mM NaCl, 300 mM sucrose, 3 mM $MgCl_2$, 1 mM EGTA] containing 0.5% Triton X-100 for 10 min on ice (41). The fixed cells were washed twice with PBS, permeabilized for 5 min with 0.5% Triton X-100 in PBS, and blocked for 30 min in 10% normal goat serum in PBS. Staining with primary antibody was performed overnight at 4°C in PBS with 0.5% goat serum. The slides were washed three times in PBS at 5-min intervals and incubated with fluorochrome-conjugated (Cy3 or Alexa Fluor 488) secondary antibodies for 30 min at room temperature in the dark. Finally, the slides were washed with PBS three times at 5-min intervals, stained with 4′,6′-diamidino-2-phenylindole (DAPI) (Molecular Probes), mounted, and examined by fluorescence microscopy. Images were visualized using an Olympus microscope and captured with a Spot Advanced imaging system.

Comet assay. DNA damage in BJ/tert fibroblast lines was determined under alkaline or neutral conditions using the CometAssay kit from Trevigen (Gaithersburg, MD) with slight modifications. Briefly, the cells were trypsinized, washed in ice-cold PBS, combined with molten agarose, and pipetted onto a comet slide. After solidification, the slides were immersed in lysis solution. For alkaline single-cell electrophoresis (detects the combination of single- and double-strand DNA breaks, DNA cross-links, and base damage), the slides were placed in alkaline buffer and electrophoresed at low voltage for 20 min at 4°C. The slides were neutralized with Tris-HCl buffer and dehydrated with 70% ethanol to fix. For neutral single-cell electrophoresis (detects only DSBs), the slides were additionally immersed in lysis solution supplemented with proteinase K. The slides were rinsed in PBS twice and placed in neutral buffer. Electrophoresis was carried out for 20 min at 10 V. Following electrophoresis, the slides were fixed as indicated above. Air-dried slides were stained with SYBR green I and analyzed by using a fluorescence microscope. The cells with damaged DNA displayed migration of DNA fragments from the nucleus, forming a tail in comet form. Comet images were captured with an Olympus microscope and Spot Advanced software. The images were analyzed using CASP software (Comet Assay Software Project 1.2.2). At least 100 comets were analyzed for each sample. Comet assays were performed three times, each time in duplicate. Differences in comet assay scored parameters were compared by analysis of variance for nonparametric values (Kruskal-Wallis test).

Viral replication assay. Viral DNA replication assays were performed as previously described (10, 22) except we used COS-1 cells, which are derived from CV-1 cells and constitutively express LT, but not a functional origin. Use of these cells resulted in optimal viability following siRNA transfection. The cells were transfected with siRNA for 48 h to ensure efficient knockdown, followed by 24 h of transfection with the SV40 origin-containing plasmid pSV01ΔEP to measure replication. The cells were harvested by scraping them into TE buffer (10 mM Tris [pH 7.5], 1 mM EDTA) containing 0.6% SDS. A small amount of the total lysate was removed for Western blot analysis. The remaining lysate was used to prepare low-molecular-weight DNA according to the Hirt protocol. Low-molecular-weight DNA was digested with DpnI restriction endonuclease to distinguish replicated DNA from input DNA and with HincII for linearization. The digested low-molecular-weight DNA was resolved on a 1.2% agarose gel, transferred to Hybond-N (Amersham Pharmacia) nylon membrane by Southern blotting, UV cross-linked, and hybridized overnight at 42°C with a ^{32}P-labeled probe prepared by random-primed labeling of the 314-bp EcoRI restriction fragment of pSV01ΔEP (Rediprime II DNA labeling system; GE Healthcare). After multiple washes, the membrane was exposed to X-ray film or a Storm Imager cassette (Molecular Dynamics).

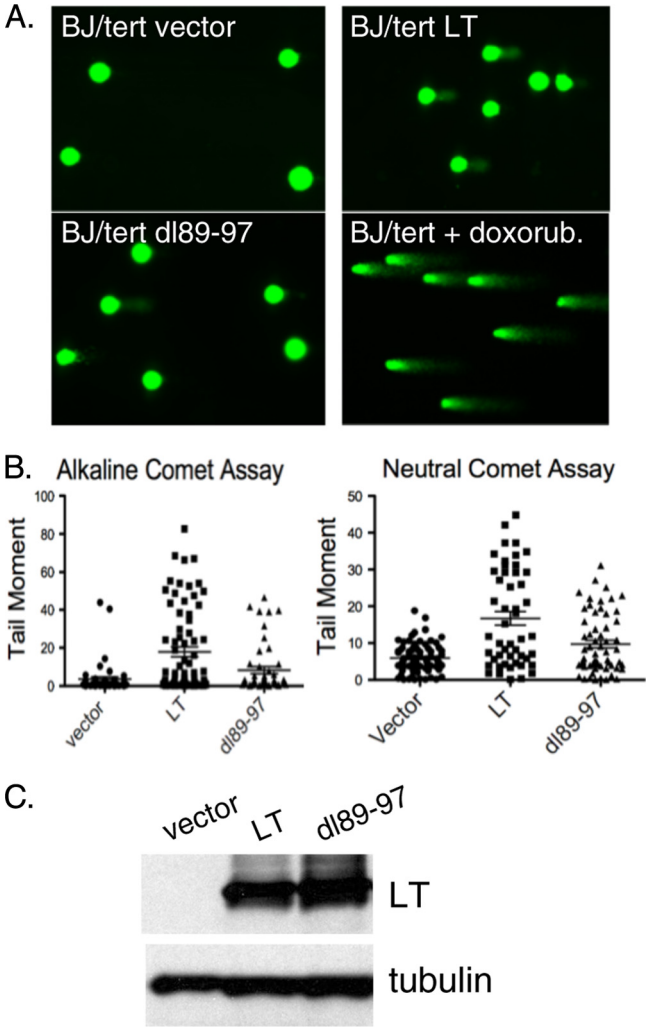

FIG. 1. Large T antigen (LT) induces DNA damage. (A) Representative images of comets from BJ/tert cells expressing an empty vector (BJ/tert vector), dl89-97 (BJ/tert dl89-97), or LT (BJ/tert LT). For a positive control, cells were treated with doxorubicin (doxorub.) for 8 h. (B) Graphic depiction of the calculated tail moment from analysis of alkaline or neutral comet assays. Data are shown for a representative experiment, where at least 100 comets were quantitated for each cell line. (C) Western blot analysis of LT and dl89-97 expression. Tubulin was included as a loading control.

RESULTS

Comet assays demonstrate that LT induces DNA damage. We previously reported that LT expression alone, in the absence of an SV40 origin of replication, induces a DDR via binding of the Bub1 mitotic checkpoint kinase (23). In this study, we extend our analysis of DDR and repair signaling in LT-expressing BJ/tert human fibroblasts as well as some of the consequences. First, we addressed whether LT induces actual DNA breakage or simply mimics it (56). This is commonly determined using a comet assay, which is based on single-cell gel electrophoresis (46). The cells are permeabilized under alkaline or neutral conditions, embedded in agarose, briefly electrophoresed at low voltage, and finally fluorescently stained with SYBR green I. If DNA breakage occurs, fragmented DNA that resembles a comet's tail can be observed. When the assay is performed under alkaline conditions, all forms of DNA damage are visualized, whereas neutral conditions allow DSBs to be distinguished. The extent of damage is frequently determined from calculations of the tail moment, which reflects both the relative amount and distribution of DNA in the tail.

We compared BJ/tert cells expressing an empty vector to derivatives stably expressing LT or the dl89-97 mutant defective in Bub1 binding (17). As a positive control, the cells were treated with the DNA-damaging agent doxorubicin. Representative comet assays are depicted in Fig. 1A. Comet tails were clearly observed for LT and the positive control, whereas cells expressing empty vector produced no comet tails and the dl89-97 mutant produced shorter tails than those seen with

wild-type LT. Quantitation of these observations is depicted in the graphs shown in Fig. 1B. The median tail moments were 17.87 (LT), 8.29 (dl89-97), and 3.58 (vector) for alkaline comet assay versus 16.71(LT), 9.71 (dl89-97), and 5.93 (vector) for the neutral comet assay. Statistical analysis was performed according to the Kruskal-Wallis test. For both alkaline and neutral conditions, the LT tail moment was significantly higher than for cells expressing empty vector and the dl89-97 mutant. Although the dl89-97 mutant was attenuated in its ability to induce DNA breakage, it consistently retained the ability to induce some degree of DNA damage. The levels of expression of LT and dl89-97 were equivalent (Fig. 1C). Since LT expression causes the appearance of comet tails also under neutral conditions, it means that DSBs are induced, which is consistent with our previous observation of ATM activation based on increased pATM S1981 signal (23). Taken together, LT does not just mimic DNA damage but induces overt DNA breakage partly in the form of DSBs, and this is partially dependent on Bub1 binding.

LT affects recruitment or retention of activated ATM at focal sites of DNA damage. We wanted to investigate the response to external damage at the single-cell level. To probe the response to DSBs, we analyzed pATM S1981 as a marker of ATM activation. As shown in Fig. 2A, BJ/tert cells expressing LT (BJ/tert LT) had significantly increased pannuclear staining for pATM S1981, whereas BJ/tert cells expressing an empty vector (BJ/tert vector) exhibited negligible background staining. While the LT-mediated increase in pannuclear staining correlated with Western blotting results for pATM S1981 (23), it was intriguing that accumulation was not focal. As expected, in response to ionizing radiation (IR), pATM S1981 in BJ/tert vector relocalized into foci that are colocalized with 53BP1 (4, 55) (Fig. 2A and B). In contrast, pATM S1981 remained pannuclear following IR treatment of BJ/tert LT cells, although 53BP1 was mobilized into foci (Fig. 2A and B). These results suggest that ATM when activated fails to be retained at DNA damage sites, which could result in an impairment of ATM signaling.

To test that hypothesis, we looked at the ATM response at 0, 2, or 24 h following 10 Gy of IR (Fig. 2C). As we previously noted, LT-expressing cells have elevated levels of pATM S1981 and pChk2 T68, whereas in cells expressing dl89-97, the levels are lower. We observed that ATM is still capable of being further activated when BJ/tert LT cells are irradiated, because pATM S1981 and pChk2 T68 increase beyond their baseline level (Fig. 2C). Interestingly, pChk2 T68 levels in LT cells continue to increase with time, peaking at 24 h, in contrast to cells expressing empty vector that have already returned to baseline levels by then. Although the ATM response appears to be intact, we cannot exclude the possibility that some substrates are affected due to the pannuclear rather than focal localization of pATM S1981.

LT activates the Fanconi anemia and HR pathways. To further delineate all the DDR and repair pathways perturbed by LT, we also investigated markers of HR (Rad51) and replication stress (FancD2) (44, 68). The FancD2 protein, a key member of the Fanconi anemia family, which responds to interstrand DNA cross-links, is activated on chromatin by monoubiquitination, thus converting it from the short (S) form to the long (L) form (44). This is often used as a surrogate marker of Fanconi anemia pathway activation (57). To assay the activation state of FancD2, we performed chromatin fractionation on BJ/tert cells expressing empty vector, BJ/tert cells expressing LT, and dl89-97 cells (Fig. 3A). Strikingly, Western blotting shows that both BJ/tert LT and dl89-97 induce the monoubiquitinated FancD2 species in the chromatin fraction (P3), whereas an empty vector does not. A perceptible increase in FancD2 levels is also observed when LT or dl89-97 is expressed; this might result from E2F-mediated transcriptional upregulation by LT (25). Similarly, both BRCA1 and Rad51 are increased (total level) and present in the chromatin fractions for LT and dl89-97, not in the vector control (Fig. 3A and B). LT and dl89-97 are expressed at similar levels, and both are present in the chromatin fraction. Orc2 was used as a marker for the chromatin fraction. To quantitate the activation state of FancD2, we determined the ratio between the long and short forms of the protein by Western blotting of RIPA whole-cell lysates (Fig. 3B). Densitometry revealed that cells expressing both LT and dl89-97 exhibit significant activation of FancD2 compared with the empty vector control.

To confirm and extend the results obtained by Western blotting, we looked by immunofluorescence for nuclear foci, another hallmark of DDR activation (5). Strikingly, LT-expressing BJ/tert cells exhibit an increased frequency of FancD2 and Rad51 foci compared to the control (Fig. 3C). The formation of Rad51 and FancD2 foci is known to occur following ionizing radiation or replication stress (5, 26, 41, 42, 51). The relative frequency of focus formation was quantitated and depicted in Fig. 3D. Approximately 80% of the cells expressing LT exhibit Rad51 foci, and this occurs independently of Bub1 binding. Similarly, LT induces foci of both FancD2 and BRCA1 in approximately 40% of the cells, again independently of Bub1 binding. LT and dl89-97 also induced a slight increase in foci of pRPA32 S4/8, believed to reflect ssDNA lesions, but the frequency was low (Fig. 3D). This RPA phosphorylation is sometimes dependent on ATR (12, 47) and may shift RPA action from cellular replication toward DNA repair (7). In all cases, the background frequency of foci was much lower. Experiments with an pRB binding-deficient mutant of LT (K1) demonstrated that binding of pocket proteins does not contribute to Rad51, FancD2, or BRCA1 focus formation (data not shown).

Colocalization studies on DDR signaling proteins in LT-expressing BJ/tert cells. In the previous section, we demonstrated that LT induces striking increases in focus formation of the Rad51, FancD2, and BRCA1 proteins, a *modus operandi* of DDR signaling molecules upon DNA damage or replication stress (5). Next, we addressed which of the relevant DDR signaling proteins are colocalized in BJ/tert LT. Notably, FancD2 and BRCA1 are highly colocalized (Fig. 4A), as previously reported for cells following genotoxic damage (21, 65). LT-expressing cells have a minor population of cells with pRPA32 S4/8 foci (Fig. 3D). When present, these were perfectly colocalized with the Rad51 recombinase (Fig. 4A). Since RPA and Rad51 have previously been reported to colocalize with PML (8), we incorporated it into our colocalization analysis. Indeed, Rad51 is colocalized with PML (Fig. 4A). The MRN complex is involved both in sensing of DSBs and in their resection to create ssDNA (5, 32). Mre11, as well as Nbs1, are

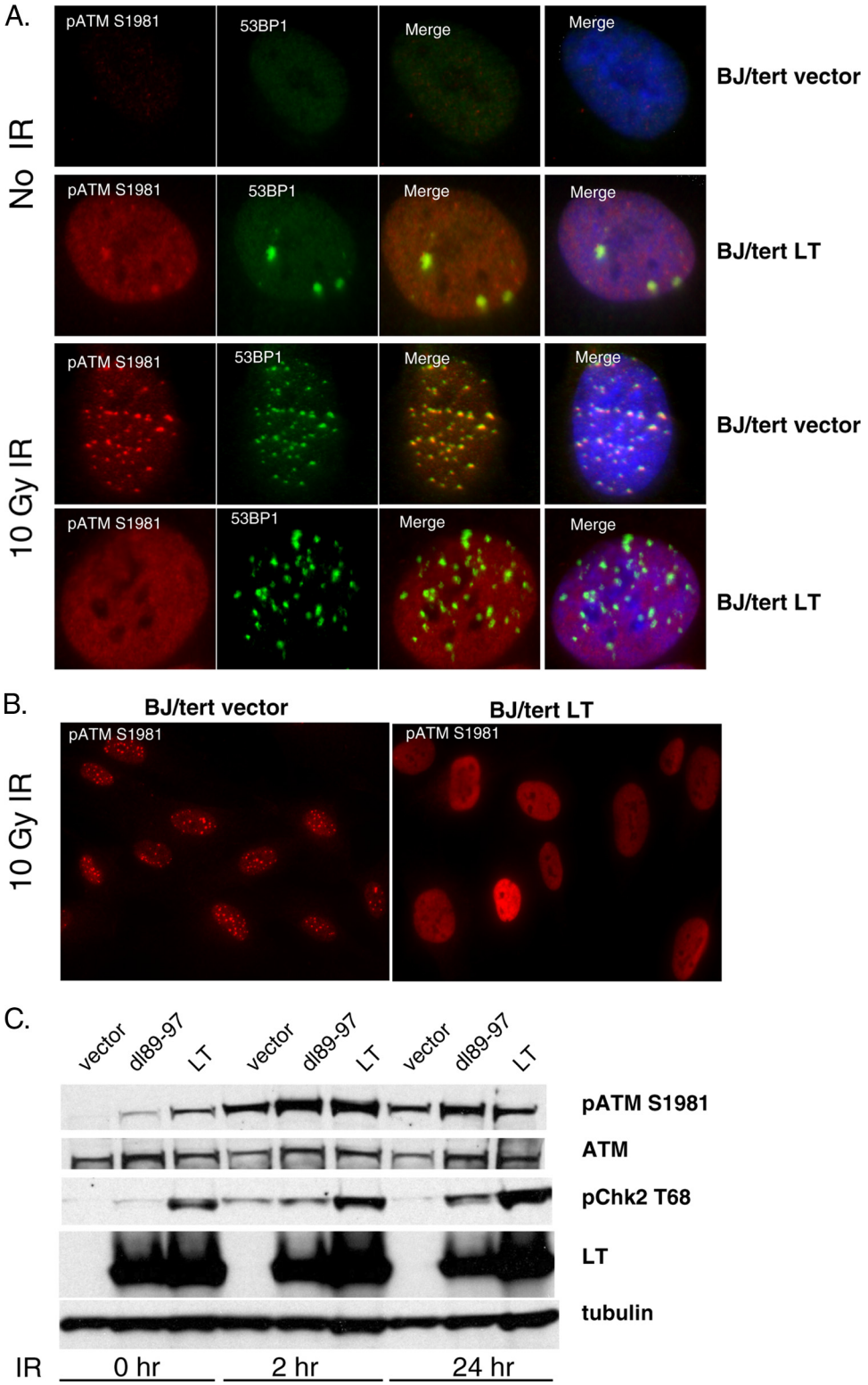

FIG. 2. LT affects the recruitment or retention of activated ATM at sites of external DNA damage. (A) BJ/tert cells expressing an empty vector (BJ/tert vector) or BJ/tert cells expressing LT (BJ/tert LT) were treated with 10 Gy of ionizing radiation (IR) or not treated with IR, allowed to recover for 5 h, and then stained by immunofluorescence for pATM S1981 and 53BP1. Merged images of the green and red channels and merged images with DAPI staining, which outlines the nucleus are also shown. (B) Whole-field images of BJ/tert vector or BJ/tert LT stained for pATM S1981 following 10 Gy of IR. (C) BJ/tert vector, BJ/tert LT, or BJ/tert dl89-97 cells were exposed to 10 Gy of IR and then analyzed by Western blotting at 0, 2, or 24 h afterwards for pATM S1981, total ATM, pChk2 T68, LT, and tubulin as a loading control.

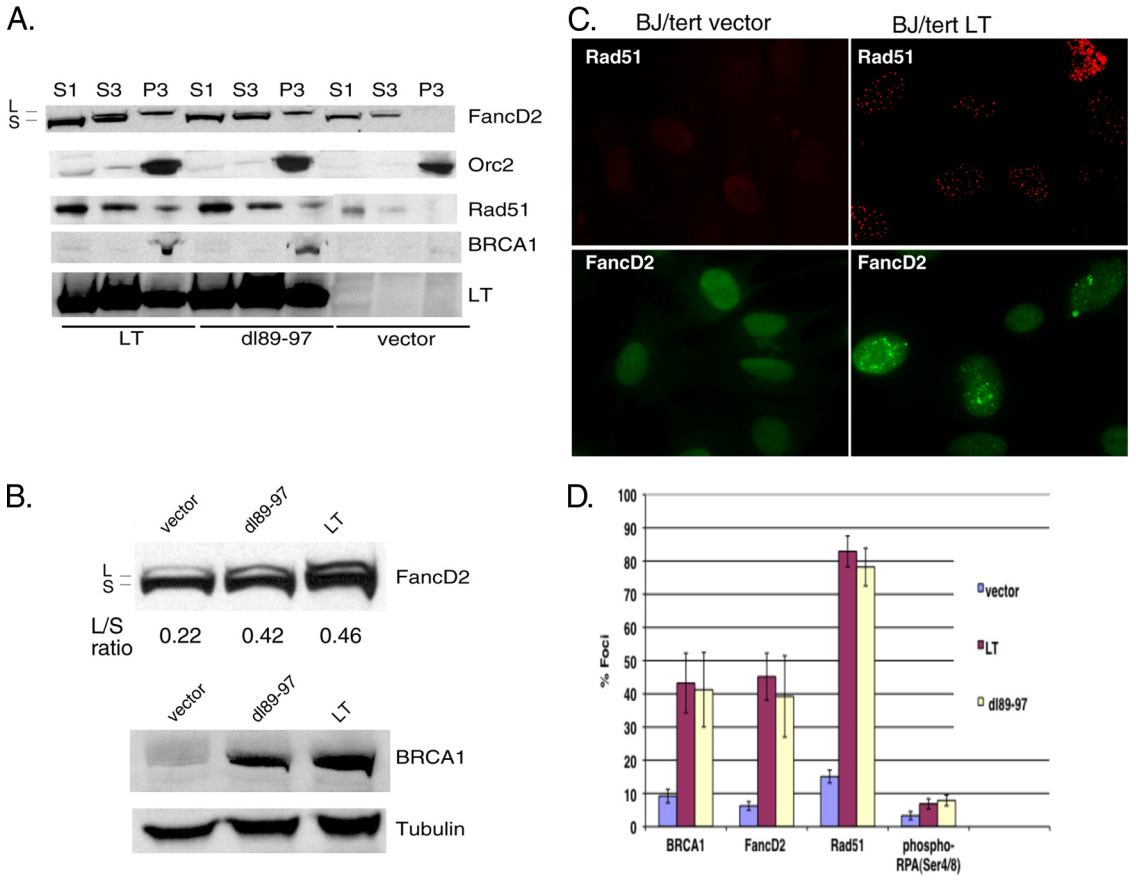

FIG. 3. LT induces the Fanconi anemia pathway and Rad51 homologous recombination (HR) foci. (A) Chromatin fractionation was performed on equivalent numbers of BJ/tert cells expressing vector, LT, or dl89-97. S1 corresponds to the cytoplasmic fraction, S3 is the soluble nuclear fraction, and P3 is the chromatin fraction. When monoubiquitinated upon activation on chromatin, FancD2 is converted from the short (S) form to the long (L) form. Western blotting was performed for FancD2, Orc2 (chromatin marker), Rad51, BRCA1, and LT. Fractionation was performed three times with similar results. (B) Radioimmunoprecipitation assay (RIPA) whole-cell lysates were analyzed for FancD2 or BRCA1 by immunoblotting. The ratio between the long and short form of FancD2 (L/S ratio) was calculated by quantitation of band intensities using ImageJ software. (C) Representative immunofluorescence images of BJ/tert vector or BJ/tert LT cells stained with either Rad51 or FancD2 antibody to monitor focus formation. (D) The relative frequency of focus formation of BRCA1, FancD2, Rad51, and pRPA (S4/8) was quantitated and depicted in a graph. At least 200 cells were counted for each condition. The values are means ± standard deviations (error bars).

colocalized with Rad51 (Fig. 4A and data not shown). PML and Nbs1 are also colocalized (Fig. 4A).

Surprisingly, we found no significant colocalization between Rad51 and FancD2 (Fig. 4A). HR is generally believed to function in repair of stalled replication forks and interstrand DNA cross-links. Indeed, FancD2 and Rad51 have been found to colocalize in some studies (65), whereas others found that FancD2 operates independently of Rad51 (45). This might reflect the unique set of DNA lesions that LT induces, or alternatively, LT is actively interfering with the assembly of DDR signaling and repair complexes, for example by blocking the recruitment of HR complexes to FancD2/BRCA1. Future studies will help to resolve whether the specific lesions defined by FancD2 immunostaining are correctly repaired. Taken together, the MRN complex, Rad51, and PML are all colocalized in BJ/tert LT, and when present, pRPA32 S4/8 is also colocalized with these. A distinct set of nuclear foci is composed of FancD2 and BRCA1. Finally, the large foci of γ-H2AX/53BP1 previously observed by us are qualitatively different from the ones studied here. Moreover, while γ-H2AX/53BP1 foci are induced by LT and 17k via Bub1 binding (23), the ones studied here are not (Fig. 3D and data not shown). There was no colocalization of 53BP1 with FancD2, but the large foci of 53BP1 were generally found in the vicinity of Rad51 foci (Fig. 4A).

DDR signaling and repair foci in LT-expressing cells are cell cycle regulated. Previous work has established that distinct repair complexes are prevalent during different stages of the cell cycle (5). In the S and G_2 phases, when sister chromatids exist as a guiding template for repair, the predominant repair mechanism is HR, whereas in G_1, it is primarily NHEJ. Some of the foci might result from replication stress, as it was previously demonstrated for various other viral oncoproteins (57, 77). We used cyclin A as a marker of S- and G_2-phase cells, since its expression level is very low in G_0/G1 (5). Dual-color immunofluorescence staining revealed that cells positive for FancD2 foci are generally also positive for cyclin A (Fig. 4B, cyclin A in red). Thus, the appearance of FancD2 foci is consistent with replication stress. Similarly, the Rad51 foci were also found primarily in S- and G_2-phase cells (cyclin A posi-

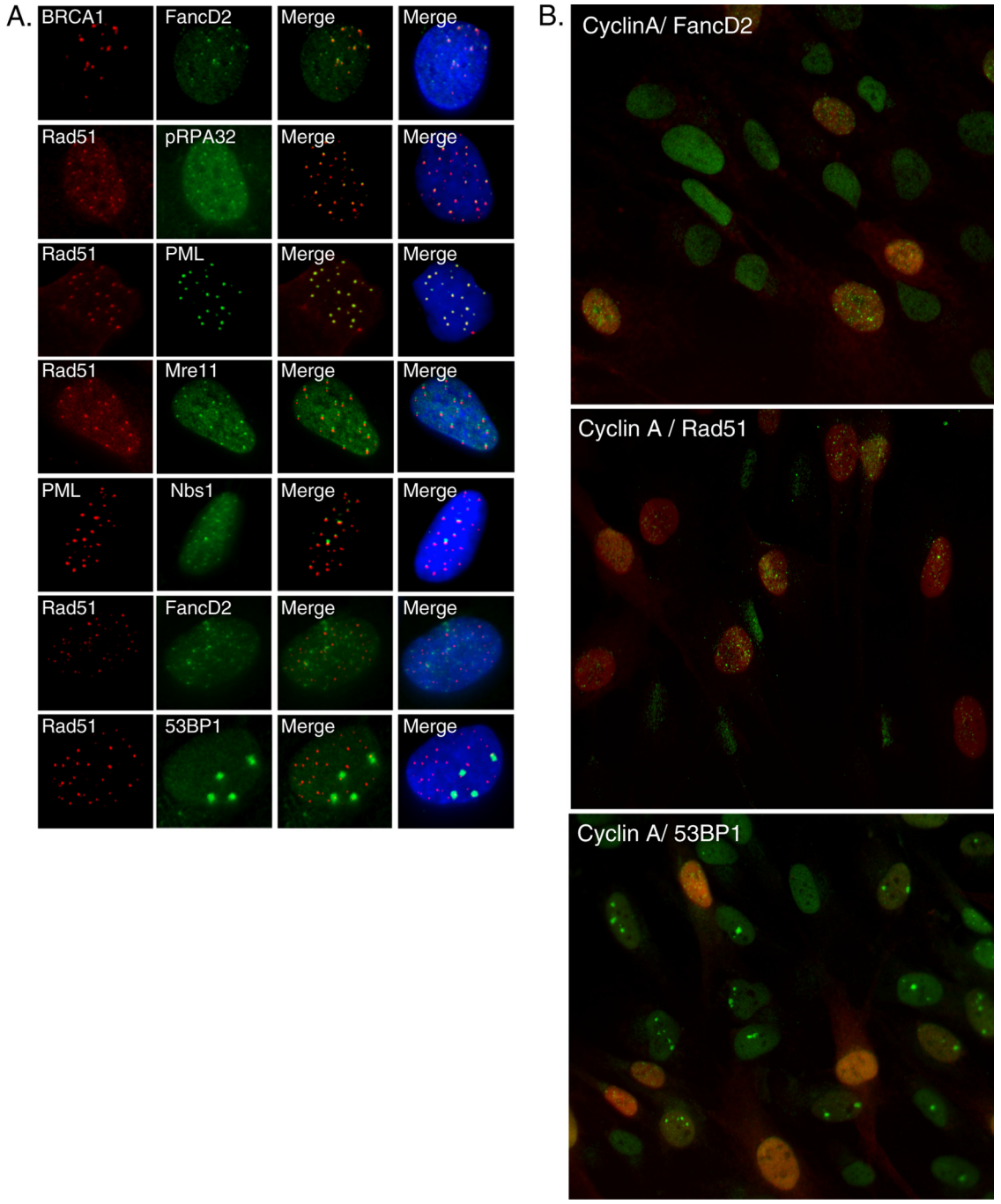

FIG. 4. Colocalization of individual LT-induced DNA damage response (DDR) signaling and repair proteins or with a marker of the cell cycle. (A) Dual-color immunofluorescence was performed on BJ/tert LT cells. The cells were stained in pairwise combinations for BRCA1, FancD2, pRPA32 S4/8, PML, Rad51, Mre11, Nbs1, and 53BP1. (B) Cyclin A (red), a marker for S/G_2-phase cells, was stained by immunofluorescence in combination with FancD2, Rad51, or 53BP1 (green). Merged images are shown. Cyclin A staining is uniformly nuclear (no foci).

tive), again suggesting replication-associated DNA damage (Fig. 4B). In contrast, when the large 53BP1 foci were analyzed for correlation with cell cycle, these were found almost always in G_1 (cyclin A-negative) cells (Fig. 4B). Collectively, our observations indicate three different categories of DDR and repair foci in BJ/tert LT. FancD2/BRCA1 and Rad51/PML/MRN constitute two cytologically distinct classes of foci that are both predominant in S/G_2. Conversely, γ-H2AX/53BP1 foci are induced by an N-terminal fragment of LT (17k) in a Bub1-dependent manner (23), and these foci are prevalent in G_1.

LT is colocalized on chromatin with a subset of DDR foci. We predicted that LT might orchestrate the appearance of some of the DDR and repair foci by direct protein-protein

interactions with one or more of the components of the foci. LT has been demonstrated to localize not just in the nucleoplasm but also on chromatin and in nuclear matrix (Fig. 3A) (60). To unmask the chromatin-localized LT population, we performed a preextraction step prior to fixation, a procedure that was previously used to visualize MRN foci after DNA damage (41). This staining procedure reveals localization of LT in nuclear foci that are in close proximity with Rad51 (Fig. 5A). Strikingly, the dl89-97 mutant fails to localize with Rad51 (Fig. 5A). Similarly, LT, but not the dl89-97 mutant, is found in close proximity with PML (Fig. 5A). This is in contrast to a previous study where localization of LT near PML bodies was contingent on a viral replication origin (64), which is absent here. While the cause of this apparent discrepancy is not clear, it is possible that our preextraction step reveals the chromatin subpopulation of LT that is juxtaposed to PML, whereas the presence of an origin relocalizes all of LT, allowing it to be visualized without preextraction. Both LT and dl89-97 are found colocalized with Nbs1 (Fig. 5A). In the minor population of cells positive for pRPA32 S4/8 foci, both LT and dl89-97 are colocalized with these foci (Fig. 5A).

Since LT was reported to bind Nbs1, we reasoned that interaction with Nbs1 might explain how LT is recruited into this class of foci (74). To test this hypothesis, we introduced LT by retroviral transfer into Nbs1-deficient GM07166 cells. Interestingly, even in the absence of functional Nbs1, LT is still found in foci localized closely with both Rad51 and PML (Fig. 5B). Therefore, LT must be recruited via an Nbs1-independent mechanism, for example by direct interaction with other repair proteins or DNA.

SV40 productive infection triggers ATR-dependent Chk1 activation and recruitment of Rad51/FancD2 into replication centers. Given our study thus far of DDR signaling and repair complexes in LT-expressing human fibroblasts, we wanted to explore the potential relevance for a productive SV40 infection. Therefore, we studied the response in BSC40 monkey kidney epithelial cells, where previously it was demonstrated that SV40 infection triggers an ATM response that facilitates the viral life cycle (54, 76). Our current observations (pRPA S4/8 and FancD2 activation [3]), as well as previous observations (23), suggested that ATR pathway activation might also occur. When analyzing SV40-infected cells 48 h postinfection by Western blotting, we found significantly increased levels of pRPA32 S4/8 and pChk1 S317, along with a substantial conversion of FancD2 to the monoubiquitinated form, compared to the results for mock-infected cells (Fig. 6A). Activation of Chk1 is dependent on ATR, since siRNA-mediated knockdown of ATR prior to infection causes pChk1 S317 to disappear. However, ATR knockdown leads only to a partial reduction in pRPA S4/8 and in the mobility shifts of total RPA and FancD2. Specific inhibition of ATM kinase with the KU55933 compound also reduced pRPA S4/8 as well as pChk1 S317. Nevertheless, we reproducibly observed reduced levels of ATR following treatment with ATM inhibitor, making it difficult to decipher the exact contribution of ATM. Treatment with ATM siRNA instead of inhibitor did not resolve this dilemma (data not shown). Equal loading was verified by blotting for tubulin. In summary, Chk1 activation clearly depends on ATR. The other DDR targets studied may be phosphorylated by both

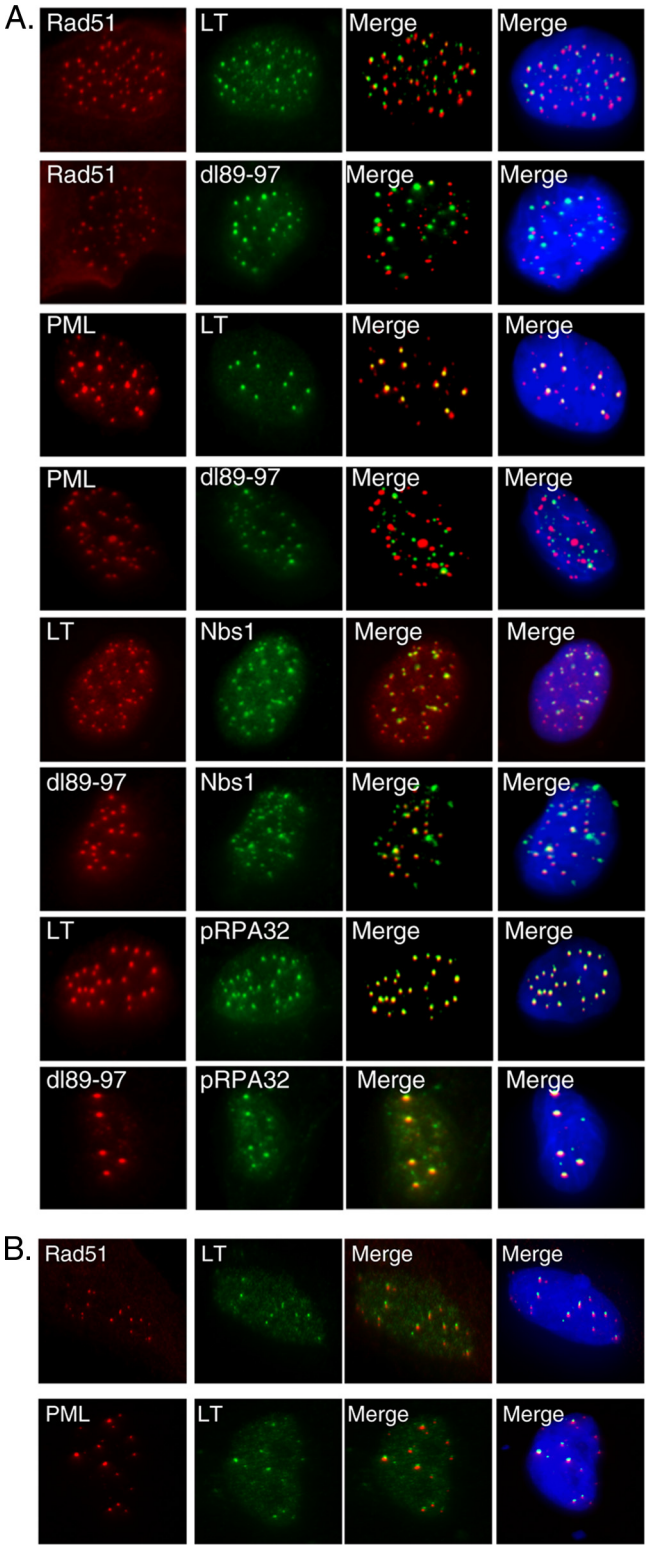

FIG. 5. Colocalization of DDR signaling and repair proteins with LT or dl89-97. Dual-color immunofluorescence labeling was performed. (A) BJ/tert cell lines were stained in pairwise combinations for LT or dl89-97 with Rad51, PML, Nbs1, or pRPA32 S4/8. (B) In GM07166 Nbs1-deficient cells, LT was costained with Rad51 or with PML.

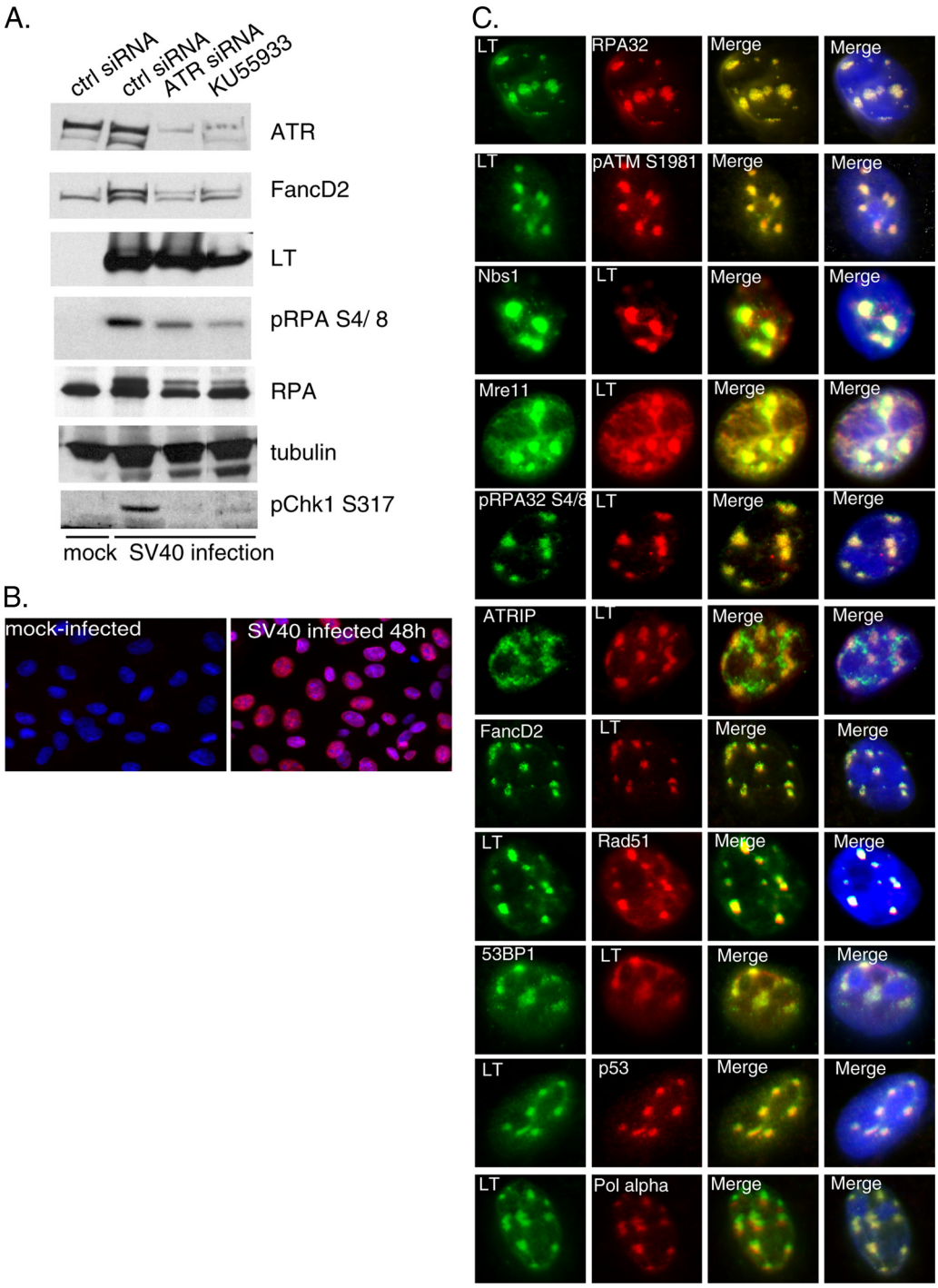

FIG. 6. SV40 infection of permissive cells induces both ATM and ATR signaling, and LT colocalizes in replication centers with multiple DDR factors. (A) BSC40 cells were transfected with control or ATR siRNA for 48 h followed by mock infection or SV40 infection for another 48 h. A specific ATM inhibitor (KU55933) was applied the last 48 h where indicated. Cells were analyzed by Western blotting for ATR, FancD2, LT, pRPA S4/8, RPA, tubulin, and pChk1 S317. (B) Expression of LT was assessed by immunofluorescence in either mock-infected or SV40-infected cells. Images were merged with DAPI staining. Nearly all cells were infected. (C) At 48 h after SV40 infection, BSC40 cells were stained by dual-color immunofluorescence. LT was examined for colocalization with RPA32, pATM S1981, Nbs1, Mre11, pRPA S4/8, ATRIP, FancD2, Rad51, 53BP1, p53, and polymerase α (Pol alpha). Identical patterns of localization were observed when LT costaining was omitted.

ATM and ATR or possibly by DNA-dependent protein kinase (DNA-PK) as well.

We also investigated whether various DDR and repair factors are recruited into viral replication centers by performing immunofluorescence on SV40-infected BSC40 cells. Single immunostaining of cells with LT antibody revealed that virtually all cells were infected (Fig. 6B). Subsequent cell staining was performed by dual-color immunofluorescence to assess colocalization with LT. As expected, on the basis of a previous study, 48 h postinfection, LT was colocalized with RPA32, pATM S1981, Nbs1, and Mre11 in large nuclear foci (Fig. 6C) (76). Consistent with the Western blotting results, we find abundant phosphorylation of RPA32 (S4/8), and the immunostaining coincides with replication centers. Repeated attempts to probe ATR localization were unsuccessful probably due to the unsuitability of antibodies for cell staining; however, ATRIP was found partially colocalized with LT. Furthermore, LT was found to be colocalized with FancD2, Rad51, 53BP1, and p53 (Fig. 6C). The observed colocalization of FancD2 and Rad51 in infected cells clearly contrasts with what we observed in BJ/tert cells expressing LT alone. The difference may be explained by the large amounts of unusual replication structures (theta-type intermediates, for example) that are produced during an SV40 infection and that are predicted to initiate DDR and repair signaling. Finally, consistent with the previous report that LT foci correspond to viral replication centers (76), we find LT colocalized with polymerase α in infected cells (Fig. 6C), whereas in noninfected cells, it was diffusively nuclear (data not shown). Whether the recruitment of a wide array of DDR and repair signaling proteins to replication centers reflects ongoing repair of SV40 genomes or whether these molecules contribute in an active way to SV40 replication, for example through HR, are important questions to be addressed.

FancD2 and Rad51 are required for efficient *in vivo* replication of an SV40 origin. To investigate the contribution of homologous recombination and repair proteins to *in vivo* viral replication, we performed transient-replication assays based on acquired resistance of a transfected SV40 origin plasmid to digestion by the DpnI restriction enzyme. We specifically depleted the relevant endogenous DDR proteins by transfection of SMARTpool siRNAs. In these studies, we found that COS-1 cells, which constitutively express LT, but not a functional SV40 origin, were optimal for preserving viability following siRNA depletion. To assay *in vivo* replication, we transfected an SV40 origin-containing plasmid for 24 h, subsequent to 48 h of siRNA-mediated silencing of DDR components.

As shown in Fig. 7A, we could readily detect the replicated form in control siRNA-transfected cells, whereas in ATM knockdown cells, replication was attenuated, consistent with several reports (18, 54, 76). Somewhat to our surprise, specific knockdown of ATR did not affect replication. It should be cautioned that ATR silencing by siRNA is never complete and related DDR kinases, like ATM or DNA-PK, might act redundantly to mask a role of ATR. However, combined knockdown with ATM and ATR siRNAs did not reduce replication further than with ATM siRNA alone (data not shown). Notably, knockdown of FancD2, and especially Rad51, significantly impaired viral replication. This suggests an important role for these factors, perhaps through repair of aberrant replication

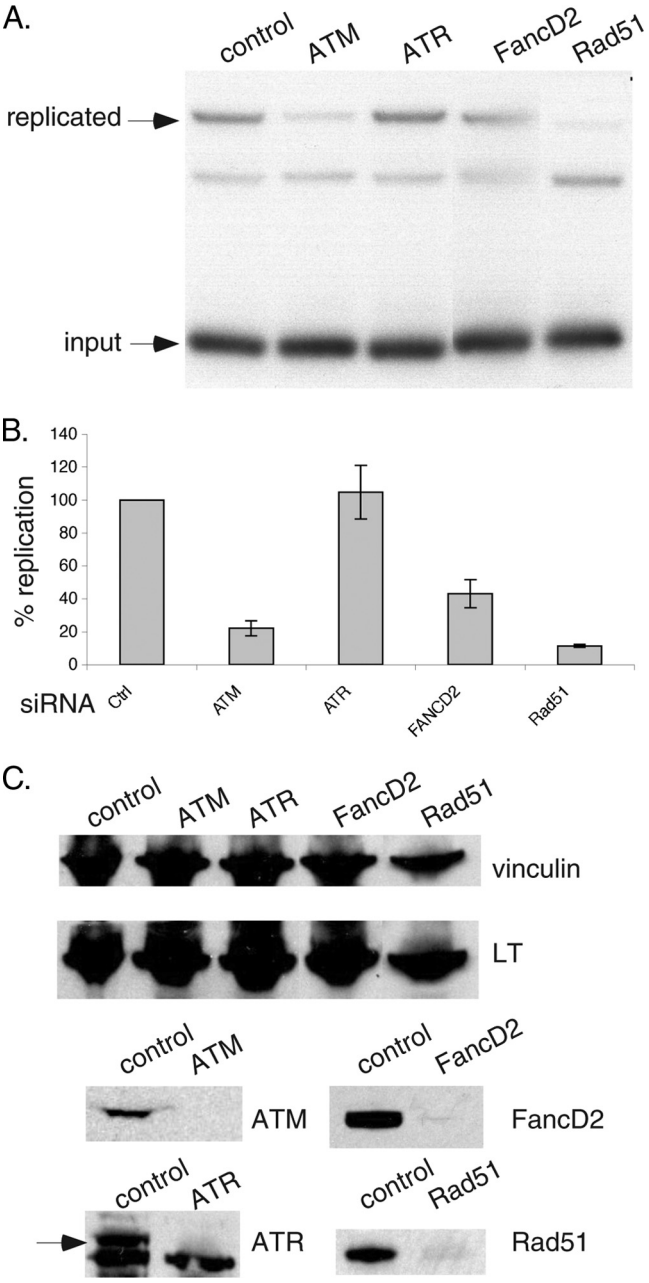

FIG. 7. FancD2 and Rad51 are required for efficient SV40 origin-dependent replication *in vivo*. (A) COS-1 cells were transfected with control, ATM, ATR, FancD2, or Rad51 siRNA for 48 h followed by 24 h of transfection with the SV40 origin-containing plasmid pSV01ΔEP. Low-molecular-weight DNA prepared according to the Hirt protocol was digested with HincII/DpnI and processed for Southern blotting analysis with an SV40 origin-specific probe. Input as well as replicated forms of DNA are indicated. (B) The signal from replicated DNA was quantitated from three independent assays. Average values along with standard deviations (error bars) are depicted in the graph. (C) Lysates from a replication assay were analyzed by Western blotting for expression of LT, vinculin (loading control), ATM, ATR, FancD2, and Rad51. As shown, siRNA-mediated depletions were efficient. The arrow indicates the mobility of ATR; the lower band is nonspecific.

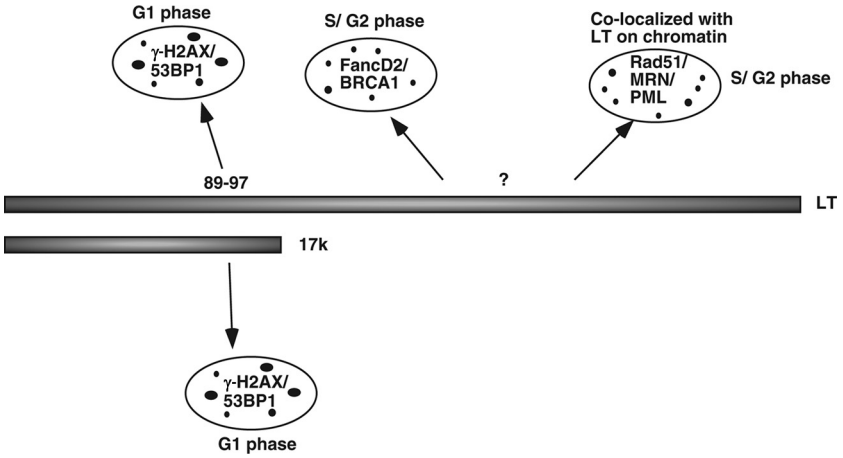

FIG. 8. Model of DDR signaling and repair pathways induced by LT. Focal accumulation of γ-H2AX/53BP1 in the G_1 phase is induced by LT, as well as 17k, via Bub1 binding to the 89-97 region of LT. In contrast, distinct foci of either FancD2/BRCA1 or Rad51/MRN/PML are prominent in S/G_2 phase. Induction of these two main classes of foci appears independent of pRB family or Bub1 binding. Only Rad51/MRN/PML are localized at, or near, LT foci. The different sized black dots for the three different categories of DDR foci reflect both the relative sizes of the foci by microscopy and their differences in spatial localization.

forms like stalled or collapsed forks. Relative replication proficiency compared with control siRNA-transfected cells was calculated by quantitation of three independent assays, and the average values with standard deviations are depicted in the graph of Fig. 7B.

To confirm the knockdown of individual DDR factors, we also performed Western blotting on the same lysates used for replication assays. As shown in Fig. 7C, all of the DDR factors were substantially depleted following siRNA transfection. Blotting with LT and tubulin antibodies further confirmed equal loading between samples. Taken together, we find that in addition to ATM, FancD2 and Rad51 also participate in SV40 origin-dependent replication *in vivo*.

DISCUSSION

Our current study has uncovered further complexities in DDR induction and regulation by LT that are important for mechanistic understanding of how LT has coopted the DDR for enhancement of viral replication (18, 23, 54, 76). Recent work has established that cellular DNA damage is not necessarily a prerequisite for a DDR (56). Importantly, our comet assay results indicate that LT is intrinsically capable of inducing DNA damage, partly in the form of DSBs. It is possible that the induction of DSBs by LT facilitates viral integration events and contributes to the previously observed promotion of gene amplification (49).

At least three distinct classes of DDR signaling and repair foci are induced by LT expression in BJ/tert cells, apparently via distinct LT domains. Our model is depicted schematically in Fig. 8. Large foci of γ-H2AX/53BP1, probably corresponding to DSBs, are induced by LT in a Bub1 binding-dependent manner (23). An pRB binding-deficient N-terminal LT fragment (17k) suffices to induce these foci (23). Since these foci are prominent in G_1 phase, they might result from errors in preceding mitotic segregation and checkpoint control, where Bub1 is primarily known to act (70). Interestingly, LT-expressing BJ/tert cells frequently exhibit chromatin bridge formation in anaphase (data not shown), which might trigger a DDR upon breakage of the DNA following cell division.

In contrast, foci of FancD2 and BRCA1 are mainly found in S/G_2 and likely connected with a replication stress response, for example from stalled or collapsed replication forks (26, 29, 44). Chromatin fractionation also indicates LT activation of FancD2. It was recently demonstrated that the human papillomavirus E7 protein, in part via pRB family binding, induces FancD2 foci and its accumulation on chromatin (57). It was further shown that E7 via a replication stress response causes alternative lengthening of telomeres (ALT)-associated promyelocytic leukemia bodies (APBs) in primary keratinocytes (58). The APBs contain FancD2, PML, and telomeric DNA. It was proposed that this induction of APBs might underlie the observed telomere maintenance, independent of telomerase, in E7-expressing cells (58). LT might similarly promote ALT via replication stress and FancD2 activation, but in our cell system (BJ/tert), this may not be relevant, since telomerase is expressed. We did not observe colocalization of the telomeric factor Trf2 with either FancD2 or PML (data not shown), suggesting that these foci do not represent APBs.

The third class of foci that LT induces is composed of the recombinase Rad51, PML, the MRN complex, and LT itself. These proteins have often been found colocalized with each other during the DDR (8, 11, 37, 73), although in some contexts it was reported that MRN and Rad51 were present in distinct types of repair foci (39). Appearance of these foci may be a result of replication-associated DNA damage that the cell is attempting to repair by HR. In the absence of functional p53, Rad51 was previously found upregulated (38, 75). Indeed, p53 can also suppress HR by direct binding to Rad51 (36). The increase in total Rad51 together with focus formation suggests an overall increase in HR, which might be correlated with the previously observed prorecombinogenic activities of LT (61, 75). However, JC polyomavirus LT modulates Rad51 in ways similar to those of SV40 but is believed to attenuate HR repair

by forcing an interaction between Rad51 and insulin receptor substrate 1 (67).

Our results from SV40 productive infection of BSC40 cells demonstrate ATR-dependent activation of Chk1. LT is colocalized during infection with phospho-RPA, ATRIP, FancD2, and Rad51. Phosphorylation of RPA is thought to act as a switch from cellular replication to DNA repair activity, consistent with the proposed concept of SV40 replication proceeding through DNA repair pathways (7, 76). Phosphorylation of RPA at S4/8 following SV40 infection is apparently mediated by both ATM and ATR. Recruitment of various repair proteins might simply reflect that the cell is detecting viral genomes as damaged DNA, but it could also be interpreted to mean that at least a subset of these repair proteins plays an active role in SV40 replication.

While we did not observe a role for ATR in SV40 origin-dependent replication *in vivo*, we conversely demonstrated that FancD2 and Rad51 play important roles. Although we do not know the precise mechanisms involved, we speculate that high-copy episomal replication with high fidelity might require the HR machinery to repair damage to the viral genome, for example because of stalled replication forks. For both herpes simplex virus type 1 (HSV-1) and Epstein-Barr virus (EBV), lytic replication also leads to recruitment of Rad51 to replication compartments; for EBV, it was demonstrated that Rad51 knockdown causes a reduction in viral genome synthesis, suggesting that HR is necessary for efficient replication (30, 69).

Notably, we found that the dl89-97 mutant fails to localize at, or near, Rad51 and PML foci, while maintaining colocalization with the MRN complex. This could be significant, since the dl89-97 mutant exhibits a defect in driving viral replication *in vivo* (data not shown). PML oncogenic domains are common targets of viruses, and polyomaviruses localize to and replicate their genomes near these structures (20, 27, 28, 64). Viral replication might be more efficient in the vicinity of these subnuclear bodies, but the underlying mechanisms have not been delineated. An intriguing possibility is that PML oncogenic domains act as master nuclear organizers for various DDR and repair factors, thereby allowing LT to target or recruit the HR machinery and facilitating repair on the viral genome (8, 28).

Why does dl89-97 fail to localize near Rad51 and PML? While we do not yet know the answer, possibilities include lack of a Bub1-mediated phosphorylation event, for example on LT, or failure to directly interact with Rad51, PML, or another component of PML oncogenic domains. The temporal assembly of DDR factors following ionizing radiation is critically dependent on phosphorylation events, for example histone H2AX phosphorylation to generate γ-H2AX generates a mark on chromatin to recruit Mdc1 and the MRN complex (63). LT might have adapted a similar mechanism for its recruitment to DDR foci. Phosphorylation of LT on S120, a proposed ATM site, is required for replication *in vivo*, thus providing a possible candidate (53, 54). Indeed, we know that specific ATM inhibition causes at least partial loss of LT localization at replication centers (76). The BRCT-related region present within the SV40 helicase domain suggests another potential mode of recruitment (31). BRCT domains, present in Mdc1 and BRCA1, are phosphoserine/threonine-dependent interaction modules important for DDR signaling (43).

What are the underlying lesions that trigger these distinct DDR and repair responses, and how are they generated? While we do not know the answer, it may be useful to first identify features or binding sites on LT that are responsible for induction of each response. The induction of both FancD2 and Rad51 foci is S/G_2 phase specific and independent of both pRB and Bub1 binding. Known LT binding partners that might be relevant for inducing these responses are Nbs1, RPA, and p53. A recent study demonstrated that JC polyomavirus LT induces an ATM/ATR-mediated G_2 checkpoint arrest by binding to cellular DNA (48). These studies make it important to investigate whether SV40 LT binding to cellular DNA, mediated by its origin-binding domain, is responsible for the observed replication stress response and either FancD2 or Rad51 focus formation. Importantly, we do not see evidence of significant G_2 accumulation when LT alone is stably expressed (data not shown), despite activation of multiple DDR and repair signaling pathways. The apparent uncoupling of DDR signaling from proper checkpoint responses may require LT interaction with additional checkpoint proteins besides p53.

Here we further show that LT induces constitutive pannuclear pATM S1981, which fails to be relocalized to foci following external DNA damage, as occurs in healthy BJ/tert cells. This suggests that LT causes a failure for ATM to be retained at sites of DNA damage, which is believed to be important for proper DDR signaling (55). Nevertheless, we did not see any significant differences in the downstream signaling events that were analyzed. It remains possible that some substrates are affected. Our observations share some similarity with the recent demonstration that HSV-1 ICP0 (infected cell polypeptide 0) by targeting cellular histone ubiquitin ligases also causes diffuse nuclear staining of pATM S1981 and its failure to be retained at repair foci (34).

Does activation of DDR and repair pathways impact LT-mediated oncogenic transformation? Multiple genetic disorders caused by DNA repair deficiency confer an increased susceptibility to cancer. Importantly, it is known that fibroblasts from individuals with Fanconi anemia are hypersensitive to SV40 transformation (66). While this observation could be related to an increased SV40 integration frequency, an alternative view is that DDR activation potentially limits SV40 oncogenic transformation, consistent with the general notion that the DDR acts as a barrier to malignancy. However, the stabilization of p53 by LT, presumably resulting from an activated DDR, can contribute to a gain of function in neoplastic transformation (9, 23, 24). The enhanced transforming ability of LT in wild-type p53 cells compared to p53-deficient counterparts is likely due to altered transcriptional patterns, perhaps because the stabilized form of p53 can recruit p300/CBP coactivators (24). Taken together, the DDR might act as a double-edged sword when modulating the LT transformation outcome. Perhaps different subsets of DDR pathways are involved in FancD2 activation versus p53 stabilization.

LT has long been known to cause structural as well as numerical chromosome instability, such as sister chromatid exchanges, dicentric chromosomes, chromosome breaks, and tetraploidy (13, 23, 72). It is possible that a links exists between perturbations of the DDR and chromosomal aberrations, but a cause-effect relationship has not been established. Future studies will be aimed at resolving these potential links between

DDR, repair, and chromosomal aberrations and illuminate how they relate to oncogenic transformation or an enhanced viral replication program.

ACKNOWLEDGMENTS

We thank Jim Pipas for kindly providing BSC40 cells, Xiaohua Wu for GM07166 cells, and Ellen Fanning for polymerase α antibody.

We gratefully acknowledge financial support from the NIH (R01 AI078926 to O.V.G.).

REFERENCES

1. **Ahuja, D., M. T. Saenz-Robles, and J. M. Pipas.** 2005. SV40 large T antigen targets multiple cellular pathways to elicit cellular transformation. Oncogene **24:**7729–7745.
2. **Ali, S. H., J. S. Kasper, T. Arai, and J. A. DeCaprio.** 2004. Cul7/p185/p193 binding to simian virus 40 large T antigen has a role in cellular transformation. J. Virol. **78:**2749–2757.
3. **Andreassen, P. R., A. D. D'Andrea, and T. Taniguchi.** 2004. ATR couples FANCD2 monoubiquitination to the DNA-damage response. Genes Dev. **18:**1958–1963.
4. **Bakkenist, C. J., and M. B. Kastan.** 2003. DNA damage activates ATM through intermolecular autophosphorylation and dimer dissociation. Nature **421:**499–506.
5. **Bekker-Jensen, S., C. Lukas, R. Kitagawa, F. Melander, M. B. Kastan, J. Bartek, and J. Lukas.** 2006. Spatial organization of the mammalian genome surveillance machinery in response to DNA strand breaks. J. Cell Biol. **173:**195–206.
6. **Bernardi, R., and P. P. Pandolfi.** 2007. Structure, dynamics and functions of promyelocytic leukaemia nuclear bodies. Nat. Rev. Mol. Cell Biol. **8:**1006–1016.
7. **Binz, S. K., A. M. Sheehan, and M. S. Wold.** 2004. Replication protein A phosphorylation and the cellular response to DNA damage. DNA Repair (Amst.) **3:**1015–1024.
8. **Bischof, O., S. H. Kim, J. Irving, S. Beresten, N. A. Ellis, and J. Campisi.** 2001. Regulation and localization of the Bloom syndrome protein in response to DNA damage. J. Cell Biol. **153:**367–380.
9. **Bocchetta, M., S. Eliasz, M. A. De Marco, J. Rudzinski, L. Zhang, and M. Carbone.** 2008. The SV40 large T antigen-p53 complexes bind and activate the insulin-like growth factor-I promoter stimulating cell growth. Cancer Res. **68:**1022–1029.
10. **Campbell, K. S., K. P. Mullane, I. A. Aksoy, H. Stubdal, J. Zalvide, J. M. Pipas, P. A. Silver, T. M. Roberts, B. S. Schaffhausen, and J. A. DeCaprio.** 1997. DnaJ/hsp40 chaperone domain of SV40 large T antigen promotes efficient viral DNA replication. Genes Dev. **11:**1098–1110.
11. **Carbone, R., M. Pearson, S. Minucci, and P. G. Pelicci.** 2002. PML NBs associate with the hMre11 complex and p53 at sites of irradiation induced DNA damage. Oncogene **21:**1633–1640.
12. **Carson, C. T., N. I. Orazio, D. V. Lee, J. Suh, S. Bekker-Jensen, F. D. Araujo, S. S. Lakdawala, C. E. Lilley, J. Bartek, J. Lukas, and M. D. Weitzman.** 2009. Mislocalization of the MRN complex prevents ATR signaling during adenovirus infection. EMBO J. **28:**652–662.
13. **Chang, T. H., F. A. Ray, D. A. Thompson, and R. Schlegel.** 1997. Disregulation of mitotic checkpoints and regulatory proteins following acute expression of SV40 large T antigen in diploid human cells. Oncogene **14:**2383–2393.
14. **Chaurushiya, M. S., and M. D. Weitzman.** 2009. Viral manipulation of DNA repair and cell cycle checkpoints. DNA Repair (Amst.) **8:**1166–1176.
15. **Chen, C., and H. Okayama.** 1987. High-efficiency transformation of mammalian cells by plasmid DNA. Mol. Cell. Biol. **7:**2745–2752.
16. **Cheng, J., J. A. DeCaprio, M. M. Fluck, and B. S. Schaffhausen.** 2009. Cellular transformation by simian virus 40 and murine polyoma virus T antigens. Semin. Cancer Biol. **19:**218–228.
17. **Cotsiki, M., R. L. Lock, Y. Cheng, G. L. Williams, J. Zhao, D. Perera, R. Freire, A. Entwistle, E. A. Golemis, T. M. Roberts, P. S. Jat, and O. V. Gjoerup.** 2004. Simian virus 40 large T antigen targets the spindle assembly checkpoint protein Bub1. Proc. Natl. Acad. Sci. U. S. A. **101:**947–952.
18. **Dahl, J., J. You, and T. L. Benjamin.** 2005. Induction and utilization of an ATM signaling pathway by polyomavirus. J. Virol. **79:**13007–13017.
19. **Dickmanns, A., A. Zeitvogel, F. Simmersbach, R. Weber, A. K. Arthur, S. Dehde, A. G. Wildeman, and E. Fanning.** 1994. The kinetics of simian virus 40-induced progression of quiescent cells into S phase depend on four independent functions of large T antigen. J. Virol. **68:**5496–5508.
20. **Everett, R. D.** 2006. Interactions between DNA viruses, ND10 and the DNA damage response. Cell. Microbiol. **8:**365–374.
21. **Garcia-Higuera, I., T. Taniguchi, S. Ganesan, M. S. Meyn, C. Timmers, J. Hejna, M. Grompe, and A. D. D'Andrea.** 2001. Interaction of the Fanconi anemia proteins and BRCA1 in a common pathway. Mol. Cell **7:**249–262.
22. **Gjorup, O. V., P. E. Rose, P. S. Holman, B. J. Bockus, and B. S. Schaffhausen.** 1994. Protein domains connect cell cycle stimulation directly to initiation of DNA replication. Proc. Natl. Acad. Sci. U. S. A. **91:**12125–12129.
23. **Hein, J., S. Boichuk, J. Wu, Y. Cheng, R. Freire, P. S. Jat, T. M. Roberts, and O. V. Gjoerup.** 2009. Simian virus 40 large T antigen disrupts genome integrity and activates a DNA damage response via Bub1 binding. J. Virol. **83:**117–127.
24. **Hermannstadter, A., C. Ziegler, M. Kuhl, W. Deppert, and G. V. Tolstonog.** 2009. Wild-type p53 enhances efficiency of simian virus 40 large-T-antigen-induced cellular transformation. J. Virol. **83:**10106–10118.
25. **Hoskins, E. E., R. W. Gunawardena, K. B. Habash, T. M. Wise-Draper, M. Jansen, E. S. Knudsen, and S. I. Wells.** 2008. Coordinate regulation of Fanconi anemia gene expression occurs through the Rb/E2F pathway. Oncogene **27:**4798–4808.
26. **Howlett, N. G., T. Taniguchi, S. G. Durkin, A. D. D'Andrea, and T. W. Glover.** 2005. The Fanconi anemia pathway is required for the DNA replication stress response and for the regulation of common fragile site stability. Hum. Mol. Genet. **14:**693–701.
27. **Ishov, A. M., and G. G. Maul.** 1996. The periphery of nuclear domain 10 (ND10) as site of DNA virus deposition. J. Cell Biol. **134:**815–826.
28. **Jul-Larsen, A., T. Visted, B. O. Karlsen, C. H. Rinaldo, R. Bjerkvig, P. E. Lonning, and S. O. Boe.** 2004. PML-nuclear bodies accumulate DNA in response to polyomavirus BK and simian virus 40 replication. Exp. Cell Res. **298:**58–73.
29. **Knipscheer, P., M. Raschle, A. Smogorzewska, M. Enoiu, T. V. Ho, O. D. Scharer, S. J. Elledge, and J. C. Walter.** 2009. The Fanconi anemia pathway promotes replication-dependent DNA interstrand cross-link repair. Science **326:**1698–1701.
30. **Kudoh, A., S. Iwahori, Y. Sato, S. Nakayama, H. Isomura, T. Murata, and T. Tsurumi.** 2009. Homologous recombinational repair factors are recruited and loaded onto the viral DNA genome in Epstein-Barr virus replication compartments. J. Virol. **83:**6641–6651.
31. **Kumar, A., W. S. Joo, G. Meinke, S. Moine, E. N. Naumova, and P. A. Bullock.** 2008. Evidence for a structural relationship between BRCT domains and the helicase domains of the replication initiators encoded by the Polyomaviridae and Papillomaviridae families of DNA tumor viruses. J. Virol. **82:**8849–8862.
32. **Lee, J. H., and T. T. Paull.** 2005. ATM activation by DNA double-strand breaks through the Mre11-Rad50-Nbs1 complex. Science **308:**551–554.
33. **Li, J. J., and T. J. Kelly.** 1984. Simian virus 40 DNA replication in vitro. Proc. Natl. Acad. Sci. U. S. A. **81:**6973–6977.
34. **Lilley, C. E., M. S. Chaurushiya, C. Boutell, S. Landry, J. Suh, S. Panier, R. D. Everett, G. S. Stewart, D. Durocher, and M. D. Weitzman.** 2010. A viral E3 ligase targets RNF8 and RNF168 to control histone ubiquitination and DNA damage responses. EMBO J. **29:**943–955.
35. **Lilley, C. E., R. A. Schwartz, and M. D. Weitzman.** 2007. Using or abusing: viruses and the cellular DNA damage response. Trends Microbiol. **15:**119–126.
36. **Linke, S. P., S. Sengupta, N. Khabie, B. A. Jeffries, S. Buchhop, S. Miska, W. Henning, R. Pedeux, X. W. Wang, L. J. Hofseth, Q. Yang, S. H. Garfield, H. W. Sturzbecher, and C. C. Harris.** 2003. p53 interacts with hRAD51 and hRAD54, and directly modulates homologous recombination. Cancer Res. **63:**2596–2605.
37. **Lombard, D. B., and L. Guarente.** 2000. Nijmegen breakage syndrome disease protein and MRE11 at PML nuclear bodies and meiotic telomeres. Cancer Res. **60:**2331–2334.
38. **Marusyk, A., L. J. Wheeler, C. K. Mathews, and J. DeGregori.** 2007. p53 mediates senescence-like arrest induced by chronic replicational stress. Mol. Cell. Biol. **27:**5336–5351.
39. **Maser, R. S., K. J. Monsen, B. E. Nelms, and J. H. Petrini.** 1997. hMre11 and hRad50 nuclear foci are induced during the normal cellular response to DNA double-strand breaks. Mol. Cell. Biol. **17:**6087–6096.
40. **Mendez, J., and B. Stillman.** 2000. Chromatin association of human origin recognition complex, cdc6, and minichromosome maintenance proteins during the cell cycle: assembly of prereplication complexes in late mitosis. Mol. Cell. Biol. **20:**8602–8612.
41. **Mirzoeva, O. K., and J. H. Petrini.** 2001. DNA damage-dependent nuclear dynamics of the Mre11 complex. Mol. Cell. Biol. **21:**281–288.
42. **Mladenov, E., B. Anachkova, and I. Tsaneva.** 2006. Sub-nuclear localization of Rad51 in response to DNA damage. Genes Cells **11:**513–524.
43. **Mohammad, D. H., and M. B. Yaffe.** 2009. 14-3-3 proteins, FHA domains and BRCT domains in the DNA damage response. DNA Repair (Amst.) **8:**1009–1017.
44. **Moldovan, G. L., and A. D. D'Andrea.** 2009. How the Fanconi anemia pathway guards the genome. Annu. Rev. Genet. **43:**223–249.
45. **Ohashi, A., M. Z. Zdzienicka, J. Chen, and F. J. Couch.** 2005. Fanconi anemia complementation group D2 (FANCD2) functions independently of BRCA2- and RAD51-associated homologous recombination in response to DNA damage. J. Biol. Chem. **280:**14877–14883.
46. **Olive, P. L., and J. P. Banath.** 2006. The comet assay: a method to measure DNA damage in individual cells. Nat. Protoc. **1:**23–29.
47. **Olson, E., C. J. Nievera, V. Klimovich, E. Fanning, and X. Wu.** 2006. RPA2

is a direct downstream target for ATR to regulate the S-phase checkpoint. J. Biol. Chem. **281:**39517–39533.
48. **Orba, Y., T. Suzuki, Y. Makino, K. Kubota, S. Tanaka, T. Kimura, and H. Sawa.** 2010. Large T antigen promotes JC virus replication in G2-arrested cells by inducing ATM- and ATR-mediated G2 checkpoint signaling. J. Biol. Chem. **285:**1544–1554.
49. **Perry, M. E., M. Commane, and G. R. Stark.** 1992. Simian virus 40 large tumor antigen alone or two cooperating oncogenes convert REF52 cells to a state permissive for gene amplification. Proc. Natl. Acad. Sci. U. S. A. **89:**8112–8116.
50. **Petrini, J. H., and T. H. Stracker.** 2003. The cellular response to DNA double-strand breaks: defining the sensors and mediators. Trends Cell Biol. **13:**458–462.
51. **Raderschall, E., E. I. Golub, and T. Haaf.** 1999. Nuclear foci of mammalian recombination proteins are located at single-stranded DNA regions formed after DNA damage. Proc. Natl. Acad. Sci. U. S. A. **96:**1921–1926.
52. **Rogakou, E. P., D. R. Pilch, A. H. Orr, V. S. Ivanova, and W. M. Bonner.** 1998. DNA double-stranded breaks induce histone H2AX phosphorylation on serine 139. J. Biol. Chem. **273:**5858–5868.
53. **Schneider, J., and E. Fanning.** 1988. Mutations in the phosphorylation sites of simian virus 40 (SV40) T antigen alter its origin DNA-binding specificity for sites I or II and affect SV40 DNA replication activity. J. Virol. **62:**1598–1605.
54. **Shi, Y., G. E. Dodson, S. Shaikh, K. Rundell, and R. S. Tibbetts.** 2005. Ataxia-telangiectasia-mutated (ATM) is a T-antigen kinase that controls SV40 viral replication in vivo. J. Biol. Chem. **280:**40195–40200.
55. **So, S., A. J. Davis, and D. J. Chen.** 2009. Autophosphorylation at serine 1981 stabilizes ATM at DNA damage sites. J. Cell Biol. **187:**977–990.
56. **Soutoglou, E., and T. Misteli.** 2008. Activation of the cellular DNA damage response in the absence of DNA lesions. Science **320:**1507–1510.
57. **Spardy, N., A. Duensing, D. Charles, N. Haines, T. Nakahara, P. F. Lambert, and S. Duensing.** 2007. The human papillomavirus type 16 E7 oncoprotein activates the Fanconi anemia (FA) pathway and causes accelerated chromosomal instability in FA cells. J. Virol. **81:**13265–13270.
58. **Spardy, N., A. Duensing, E. E. Hoskins, S. I. Wells, and S. Duensing.** 2008. HPV-16 E7 reveals a link between DNA replication stress, Fanconi anemia D2 protein, and alternative lengthening of telomere-associated promyelocytic leukemia bodies. Cancer Res. **68:**9954–9963.
59. **Srinivasan, A., A. J. McClellan, J. Vartikar, I. Marks, P. Cantalupo, Y. Li, P. Whyte, K. Rundell, J. L. Brodsky, and J. M. Pipas.** 1997. The amino-terminal transforming region of simian virus 40 large T and small t antigens functions as a J domain. Mol. Cell. Biol. **17:**4761–4773.
60. **Staufenbiel, M., and W. Deppert.** 1983. Different structural systems of the nucleus are targets for SV40 large T antigen. Cell **33:**173–181.
61. **St-Onge, L., L. Bouchard, S. Laurent, and M. Bastin.** 1990. Intrachromosomal recombination mediated by papovavirus large T antigens. J. Virol. **64:**2958–2966.
62. **Stracker, T. H., C. T. Carson, and M. D. Weitzman.** 2002. Adenovirus oncoproteins inactivate the Mre11-Rad50-NBS1 DNA repair complex. Nature **418:**348–352.
63. **Stucki, M., and S. P. Jackson.** 2006. γH2AX and MDC1: anchoring the DNA-damage-response machinery to broken chromosomes. DNA Repair (Amst.) **5:**534–543.
64. **Tang, Q., P. Bell, P. Tegtmeyer, and G. G. Maul.** 2000. Replication but not transcription of simian virus 40 DNA is dependent on nuclear domain 10. J. Virol. **74:**9694–9700.
65. **Taniguchi, T., I. Garcia-Higuera, P. R. Andreassen, R. C. Gregory, M. Grompe, and A. D. D'Andrea.** 2002. S-phase-specific interaction of the Fanconi anemia protein, FANCD2, with BRCA1 and RAD51. Blood **100:**2414–2420.
66. **Todaro, G. J., H. Green, and M. R. Swift.** 1966. Susceptibility of human diploid fibroblast strains to transformation by SV40 virus. Science **153:**1252–1254.
67. **Trojanek, J., S. Croul, T. Ho, J. Y. Wang, A. Darbinyan, M. Nowicki, L. Del Valle, T. Skorski, K. Khalili, and K. Reiss.** 2006. T-antigen of the human polyomavirus JC attenuates faithful DNA repair by forcing nuclear interaction between IRS-1 and Rad51. J. Cell. Physiol. **206:**35–46.
68. **West, S. C.** 2003. Molecular views of recombination proteins and their control. Nat. Rev. Mol. Cell Biol. **4:**435–445.
69. **Wilkinson, D. E., and S. K. Weller.** 2004. Recruitment of cellular recombination and repair proteins to sites of herpes simplex virus type 1 DNA replication is dependent on the composition of viral proteins within prereplicative sites and correlates with the induction of the DNA damage response. J. Virol. **78:**4783–4796.
70. **Williams, G. L., T. M. Roberts, and O. V. Gjoerup.** 2007. Bub1: escapades in a cellular world. Cell Cycle **6:**1699–1704.
71. **Wobbe, C. R., F. Dean, L. Weissbach, and J. Hurwitz.** 1985. In vitro replication of duplex circular DNA containing the simian virus 40 DNA origin site. Proc. Natl. Acad. Sci. U. S. A. **82:**5710–5714.
72. **Woods, C., C. LeFeuvre, N. Stewart, and S. Bacchetti.** 1994. Induction of genomic instability in SV40 transformed human cells: sufficiency of the N-terminal 147 amino acids of large T antigen and role of pRB and p53. Oncogene **9:**2943–2950.
73. **Wu, G., X. Jiang, W. H. Lee, and P. L. Chen.** 2003. Assembly of functional ALT-associated promyelocytic leukemia bodies requires Nijmegen breakage syndrome 1. Cancer Res. **63:**2589–2595.
74. **Wu, X., D. Avni, T. Chiba, F. Yan, Q. Zhao, Y. Lin, H. Heng, and D. Livingston.** 2004. SV40 T antigen interacts with Nbs1 to disrupt DNA replication control. Genes Dev. **18:**1305–1316.
75. **Xia, S. J., M. A. Shammas, and R. J. Shmookler Reis.** 1997. Elevated recombination in immortal human cells is mediated by HsRAD51 recombinase. Mol. Cell. Biol. **17:**7151–7158.
76. **Zhao, X., R. J. Madden-Fuentes, B. X. Lou, J. M. Pipas, J. Gerhardt, C. J. Rigell, and E. Fanning.** 2008. Ataxia telangiectasia-mutated damage-signaling kinase- and proteasome-dependent destruction of Mre11-Rad50-Nbs1 subunits in simian virus 40-infected primate cells. J. Virol. **82:**5316–5328.
77. **Zimmerman, E. S., M. P. Sherman, J. L. Blackett, J. A. Neidleman, C. Kreis, P. Mundt, S. A. Williams, M. Warmerdam, J. Kahn, F. M. Hecht, R. M. Grant, C. M. de Noronha, A. S. Weyrich, W. C. Greene, and V. Planelles.** 2006. Human immunodeficiency virus type 1 Vpr induces DNA replication stress in vitro and in vivo. J. Virol. **80:**10407–10418.